Development of a low-cost piezo film-based knock sensor

DOI: 10.1243/09544070360692087

E Pipitone* and **L D'Acquisto**
Dipartimento di Meccanica, University of Palermo, Palermo, Italy

Abstract: It is well known that spark advance is a key parameter in spark ignition engine management. Increasing fuel cost and emission regulation strictness require a higher engine efficiency, which can be improved by an accurate regulation of the spark advance. Under high load conditions, an optimal spark advance choice leads the engine to run next to the knock limit, so the management and control system needs to be equipped with a knock sensor in order to preserve the engine from damage. The authors developed a low-cost knock sensor whose sensing element is a thin washer of polyvinylidine fluoride (PVDF), a fluoropolymer characterized by a great piezoelectric effect if polarized. The sensor has been tested on a spark ignition CFR engine (the standard single-cylinder test engine used by ASTM for octane number determination of spark ignition engine fuel) and compared with a commercial accelerometer and a pressure sensor, in terms of knocking detection capability, measured knock intensity (KI) and signal-to-noise ratio (SNR). Knocking tests have also been carried out on a Renault series production engine. The collected data show that PVDF ensures a reliable detection of knock, a precise measurement of knock energy and accurate information about the frequency content of the perceived vibration. The sensor worked for several hours without depolarizing and, above all, owing to the great piezoelectric effect of PVDF, the use of a charge amplifier was unnecessary. PVDF proved to have great potential as a knock detector in spark ignition engines at a very low cost.

Keywords: knock sensor, spark advance control, spark ignition engine, piezo film

NOTATION

CA	crank angle
ECU	electronic control unit
IAV	integral of the absolute value
IFD	integral of the first derivative absolute value
KI	knock intensity
KIR	knock intensity ratio
MBT	maximum brake torque
MFD	maximum first derivative
PPV	peak-to-peak value
PVDF	polyvinylidine fluoride
RMS	root mean square
RPM	revolution per minute
SNR	signal-to-noise ratio
WOT	wide-open throttle (full load condition)

The MS was received on 13 February 2003 and was accepted after revision for publication on 6 March 2003.
* *Corresponding author: Dipartimento di Meccanica, Viale delle Scienze, University of Palermo, Palermo, 90128, Italy. email: pipitone@dima.unipa.it*

1 INTRODUCTION

Today's spark ignition engines need very accurate spark advance regulation to improve efficiency [**1**–**7**]. The spark advance control can be either in open or in closed loop, the second being more effective in reducing fuel consumption; an accurate control of spark advance (maximum brake torque timing) can cause knocking, an abnormal combustion phenomenon that can seriously damage the engine, so the ECU cannot operate without a knock control system in order to prevent engine failure. A modern, on-board, real-time knock control system needs a sensor that fulfils certain requirements: it must be compact, cheap and easy to install, and must ensure reliable knock detection and quantification. Nowadays, two kinds of sensor are mostly used in knock control systems: the pressure sensor and the accelerometer. The first measures in-cylinder pressure, showing pressure oscillation due to knocking. High costs (especially for multiple-cylinder monitoring) and mounting difficulties (the pressure sensor must be in direct communication with the combustion chamber) are the drawbacks of such a sensor; moreover, piezoelectric pressure transducers require the use of a charge amplifier, and, as far as knocking detection is concerned, a frequency filter too; the filtered pressure signal reveals knock occurrence immediately and with good accuracy.

The second kind of sensor, the accelerometer, measures structure-borne noise at the engine block, generating an electrical signal whose amplitude depends on the intensity of the perceived vibration; the resulting vibration signal is composed of mechanical noise (due to valve closing and piston slap) and knocking noise, and, especially at high engine speed, the first can be superimposed on the second, so these sensors may suffer from a poor signal-to-noise ratio (SNR). For knocking detection purposes, this kind of sensor presents some advantages in comparison with the pressure sensor, which makes it affordable both for series production engines and for R&D: ease of installation, lower cost and the possibility of being used without a frequency filter. In this case the knock detection technique relies on the amplitude of the signal generated by the sensor, or on other knock intensity related parameters derived from the unfiltered signal analysis [**7**, **8**]. In some cases, knock detection has also been performed by ion current sensing [**9**].

Knock detection techniques based on the use of accelerometers are almost identical to those based on pressure signal analysis and can be divided into two categories: time-based analysis (the knock intensity is calculated from an analysis of the filtered or unfiltered signal over time) and frequency-based analysis (knock occurrence is revealed by means of signal analysis in the frequency domain). The latter presents some difficulties related both to the presence of several knocking frequencies (owing to the presence of several pressure oscillation modes in the combustion chamber) and to knocking frequency variation with load and crank angle (i.e. with combustion chamber temperature and volume), as shown by Draper's equation [**10**–**13**].

To account for this variation, many authors have adopted the joint time–frequency analysis technique, which improves the SNR but requires heavier calculations [**13**–**18**], so it is not suitable for on-board, real-time knock control. In this work, the authors decided to perform time-based analysis for knock energy measurement.

1.1 Piezo film based knock sensor

Standard accelerometers used in automotive engines for knock detection are made of a piezoceramic sensing element that measures inertial forces exerted by a seismic mass, excited by the vibration generated by knocking and transmitted through the engine block [**3**]. The choice of piezo film as the sensing element for the realization of knock sensors has not been investigated in the recent past, and at present there is no evidence of commercial knock detectors based on this material. The chosen piezo film, a copolymer of polyvinylidene fluoride (PVDF) called P(V2F-V3F) and Pt + Au plated on both surfaces, makes it possible to realize a tailored knock sensor operating in mode 33.

Copolymers have recently been commercialized with a depolarizing temperature above 130 °C and recommended use with a maximum temperature of 110 °C. This enables its use outside the engine block under working conditions which are the same as those of commercial accelerometers. The nominal characteristics of the film, according to the data provided by the supplier Piezotech SA, are as follows: thickness 100 μm; $d_{33} = 24–30$ pC/N m^2.

The low thickness allows a very compact construction of sensors based on this material, while the high sensitivity d_{33} (which indicates piezo activity of the film along the thickness axis and corresponds to the electrical charges delivered by 1 m^2 when it is exposed to a pressure of 1 Pa along this axis) makes this material applicable for the realization of a knock sensor with a high-level output signal that does not need further amplification. The bandwidth signal of a typical knock event, according to Draper's equation, was initially considered in the region 5–25 kHz; the corresponding dynamic range of the PVDF-based sensor was obtained with a seismic mass of a few grammes. As far as the design of the transducer is concerned, an annular layout was chosen with an outer diameter adequate to ensure simple positioning on the lateral surface of the engine block, close to the cylinder head.

The piezo film based knock sensor was built following the above-illustrated principle, and, as shown in Fig. 1 and in the three-dimensional model presented in Fig. 2, it is equipped with a seismic mass, which transmits

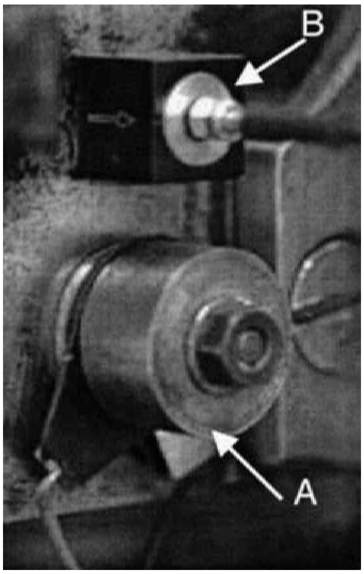

Fig. 1 PVDF knock sensor (A) and commercial accelerometers (B) bonded on the engine block

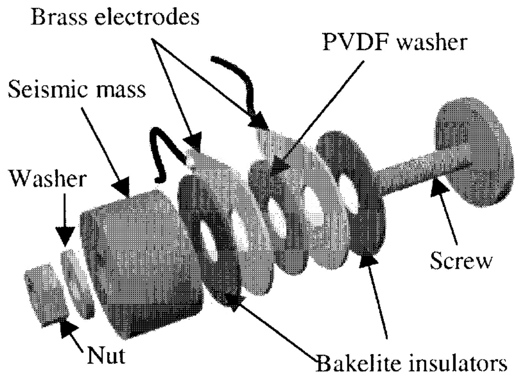

Fig. 2 PVDF knock sensor three-dimensional model

engine block vibration to a thin PVDF washer that is Pt + Au metallized on both sides and clamped between two brass electrodes and two disc-shaped bakelite elements, used for electrical insulation; the whole was locked by a bolt, whose flat head surface was bonded on the engine block using a common cyanoacrylate adhesive.

The realized knock sensor was compact and space saving, with an outer diameter and overall height of 17 mm. Useful information and typical properties of piezo films can be found from Measurement Specialties Incorporated [**19**] or Piezotech SA (www.piezotech.fr).

One of the characteristics that makes PVDF particularly suitable for knock detection is the relatively high voltage field generated by mechanical stress, which makes a charge amplifier unnecessary for knock measurement requirements. This contributes to lower PVDF cost as a knock sensor.

The first stage of the tests was conducted with an annular PVDF sensor with an internal diameter of 6 mm and an external diameter of 16 mm and with a seismic mass of $4 \pm 0.5 \times 10^{-3}$ kg (test 1) and $9 \pm 0.5 \times 10^{-3}$ kg (test 2).

The axial preload of the mass, approximately 2 kN, proved to be adequate both to avoid damage to the film and to leave the mass loose.

The signal amplitude of measured knocking events showed an appreciable linear dependence on the amplitude of the seismic mass mounted. On the basis of this result, a mass with an amplitude of $15 \pm 0.5 \times 10^{-3}$ kg was used in the following experimental tests.

2 EXPERIMENTAL TESTS ON THE CFR ENGINE

In order to evaluate PVDF knock detection performance with respect to a pressure sensor and a commercial accelerometer, some comparative tests have been carried out [**20**] on a spark ignition CFR engine, the standard single-cylinder engine used for gasoline octane rating (see ASTM D2699 and D2700 standard test method [**21**]); its basic characteristics are given in Table 1.

The experimental set-up was equipped with:

(a) a spark ignition CFR engine running at a fixed compression ratio of 9 and fuelled with RON 95 unleaded gasoline;
(b) a commercial Brüel & Kjær Cubic DeltaTron accelerometer of type 4502 (B in Fig. 1) with a constant current supplier of type WB 1372;
(c) a PVDF-based knock sensor (A in Fig. 1);
(d) a Kistler pressure sensor 7055B with a charge amplifier of type 5001;
(e) an Agilent 54624A 100 MHz digital oscilloscope with four analogue channels;
(f) a K-type thermocouple to monitor engine temperature;
(g) a PC equipped with LabView software for data analysis.

At a fixed compression ratio, knocking was induced, advancing spark ignition, thus obtaining incipient, normal or heavy knocking conditions. The signals generated by the three sensors were displayed on the digital oscilloscope and saved as numerical data at a sampling frequency of 100 kHz; the collected data were used to perform frequency analysis and knocking intensity evaluation using LabView software.

The oscilloscope bandwidth was limited to 20 MHz in order to filter high-frequency noise. As regards the main resonant knocking frequency, a value between 5 and 10 kHz was expected both from the literature [**1**, **5**, **9**–**12**, **14**, **15**, **22**–**24**] and from Draper's equation [**13**]

$$f = \frac{k_{1,0,0} C_s}{\pi B} \tag{1}$$

where $k_{1,0,0} = 1.841$ is the wave number for the first radial mode of vibration, C_s is the speed of sound (approximately 900 m/s considering a temperature of 2000 K) and $B = 82.55$ mm is the engine bore. The equation yields $f = 6.3$ kHz, and in fact the power spectrum of the pressure signal, filtered by a 3 kHz high-pass filter (Fig. 3), confirmed the main knocking frequency of the CFR engine to be about 6 kHz. Therefore, in order to remove background noise, each signal has been filtered by a fourth-order Butterworth 5–10 kHz bandpass filter.

Figure 4 shows the power spectra of the bandpass filtered signals from the three sensors: it is clear that, for

Table 1 CFR spark ignition engine characteristics

Bore	82.55 mm
Stroke	114.3 mm
Displacement	611 cm^3
Compression ratio range	3.5:1–18:1

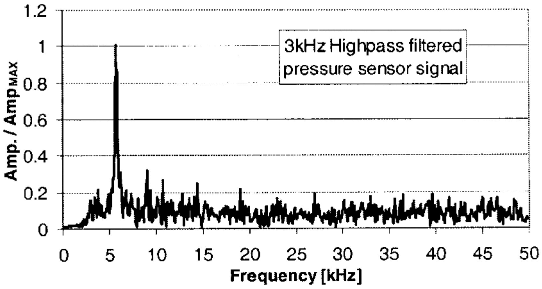

Fig. 3 Power spectrum of the 3 kHz high-pass filtered pressure signal: the main CFR engine knocking is about 6 kHz

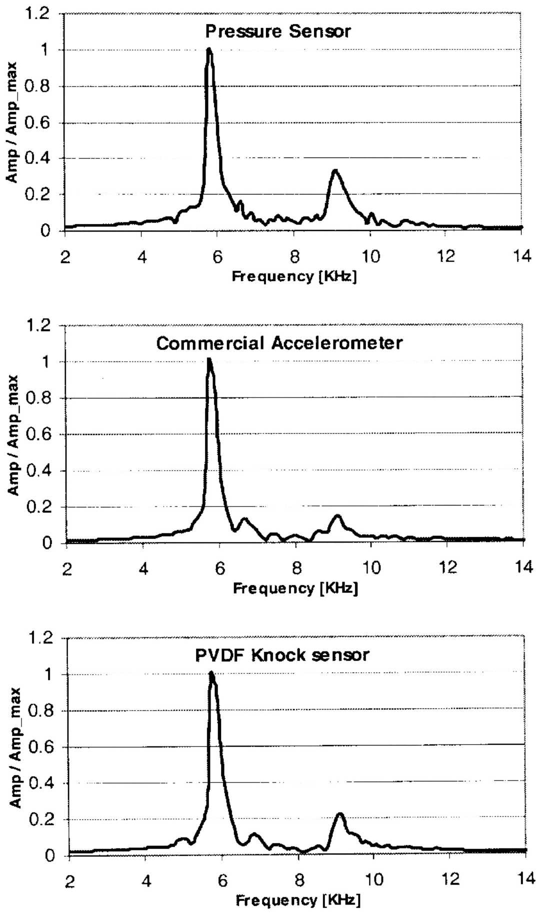

Fig. 4 Power spectra of 5–10 kHz bandpass filtered signals

frequency analysis matters, the three sensors give the same information.

The data saved by the oscilloscope were used to perform knock intensity evaluation and comparison; no standard has been found in the literature for knock energy measurement, so the authors decided to evaluate knock intensity by means of five different definitions [**11**, **23**, **24**]:

1. Peak-to-peak value

$$\mathrm{PPV} = \max(\boldsymbol{X}) - \min(\boldsymbol{X})$$

2. Maximum absolute value of the first derivative

$$\mathrm{MFD} = \max\left|\frac{\mathrm{d}X}{\mathrm{d}t}\right|$$

3. Root mean square

$$\mathrm{RMS} = \sqrt{\frac{1}{N}\sum_{i=1}^{N} X_i^2}$$

4. Integral of the absolute value of the first derivative

$$\mathrm{IFD} = \int \left|\frac{\partial X}{\partial t}\right| \mathrm{d}t$$

5. Integral of the absolute value

$$\mathrm{IAV} = \sum_{1}^{N} |\mathrm{X}_i|$$

where $\boldsymbol{X}$ is the N-dimensional vector containing the acquired vibration data X_i ($\forall\, i = 1, \ldots, N$).

The five above-mentioned knock intensity definitions can be divided into two categories: the first, to which PPV and MFD belong, measures knock-related energy by means of a small portion of the sampled data; the second, to which RMS, IFD and IAV belong, evaluates knock intensity using the whole sampled data. As will be shown below, the results obtained point out this subdivision.

Knock intensity (KI) was calculated on the basis of the 5–10 kHz bandpass filtered data obtained from each sensor. The data were sampled at a 100 kHz frequency, and an observation window of 50° crank angle (CA) was chosen [**10**, **11**, **13**, **24**], starting the measurement at the onset of knocking.

The comparison of sensor performance is made in terms of relative KI, i.e. the ratio between the KI value and the maximum measured KI. Figure 5 shows the results of the comparison test on the CFR engine between the PVDF knock sensor and the commercial accelerometer (52 knocking cycles): for each KI definition, a diagram reports the PVDF relative KI versus the commercial accelerometer relative KI. The data reveal a good correlation.

Table 2 gives a summary of the comparison knocking test between the PVDF sensor and the accelerometer; in this table, the first row shows the knock intensity ratio (KIR), which is the mean value of the ratio between the two measured knock intensities: the PVDF KI varied from 55 to 47 per cent of the KI measured by the commercial accelerometer.

Knock intensity evaluation alone is not meaningful for sensor comparison purposes, so the SNR for each sensor has been evaluated, sampling and analysing the background noise in the same observation window (50° CA).

The second row of Table 2 reports the ratio of PVDF SNR to accelerometer SNR: the PVDF knock sensor exhibits a 21 to 66 per cent higher SNR with respect to

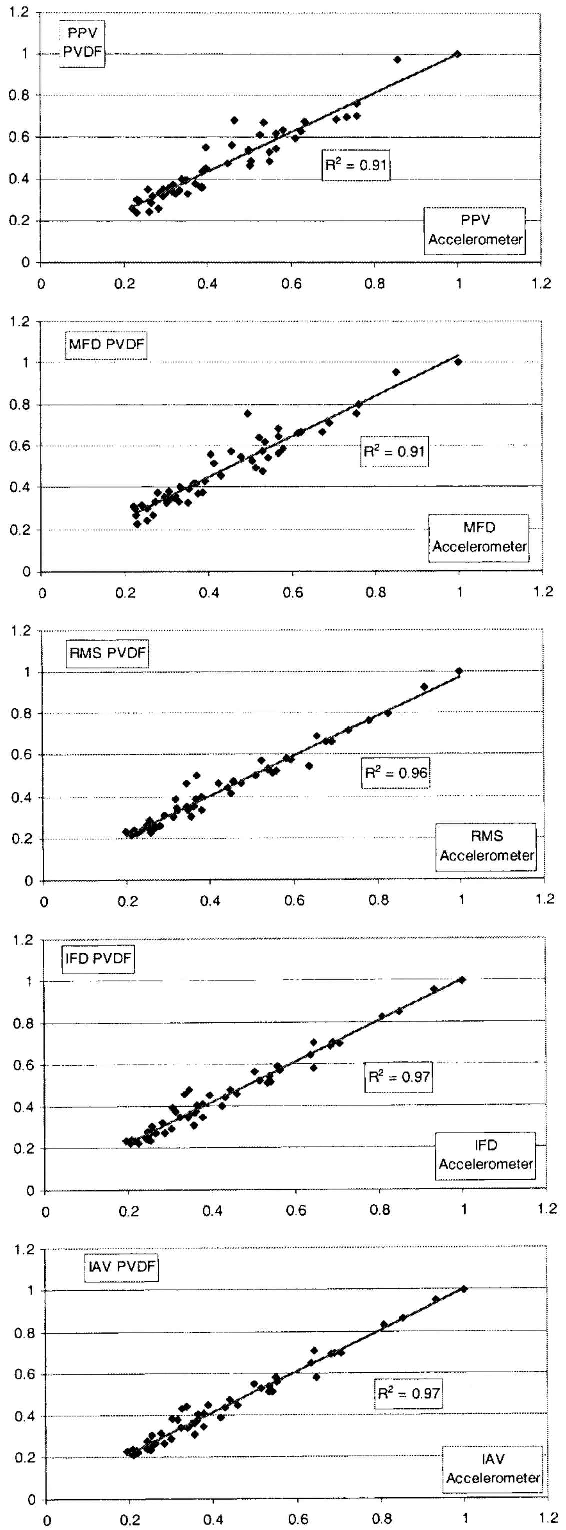

Fig. 5 PVDF knock sensor versus commercial accelerometer: comparison results

the commercial accelerometer. This is an encouraging result, since the PVDF knock sensor has been used without any charge amplifier, and its total cost is estimated to be lower than 10 Euro. In the last row of Table 2 the correlation factor between PVDF KI and commercial accelerometer KI is reported.

Table 2 Summary of the comparison test between the PVDF sensor and the commercial accelerometer

	PPV	MFD	RMS	IFD	IAV
Mean KIR	0.55	0.55	0.49	0.48	0.47
SNR ratio	1.64	1.66	1.33	1.25	1.21
Correlation	0.91	0.91	0.96	0.97	0.97

Figure 6 and Table 3 show the results of the comparative test between the PVDF knock sensor and the pressure sensor on the CFR engine: this time, slightly poorer correlation was found, above all for PPV and MFD criteria.

On the whole, the PVDF knock sensor proved to be really competitive both in knocking detection and in KI measurement compared with the commercial accelerometer and the pressure sensor. The tested PVDF knock sensor worked for several hours bonded on the engine block, reaching a temperature of 90 °C without depolarizing, and, unlike the commercial accelerometer and the pressure sensor, it never appeared to suffer from thermal drift.

Tables 2 and 3 clearly show up the above-mentioned evaluation criteria subdivision into two categories: in fact the criteria that evaluate KI on the basis of a small portion of the sampled signal (poor information), PPV and MFD, obtained a moderate correlation, while those criteria of KI evaluation that take into account the whole sampled signal (complete information), RMS, IFD and IAV, reached a higher correlation factor

3 EXPERIMENTAL TESTS ON THE SERIES PRODUCTION ENGINE

In order to verify the results obtained with the CFR engine on an actual automotive engine, a further experimentation has been carried out on a test bench equipped with a Renault four-cylinder, 1598 cm^3, 16-valve, multipoint spark ignition engine connected to an eddy current dynamometer. The use of a pressure sensor was not possible this time, so the comparative test involved only the PVDF knock sensor and the commercial accelerometer, both of them bonded on the engine block, between cylinders 2 and 3.

The tests were conducted at 1500 and 3000 r/min, and at fixed load (approximately 0.85 WOT). Knocking was induced alternately in cylinder 2 or 3, advancing the spark timing and slightly leaning the mixture.

The image taken by the oscilloscope and reported in Fig. 7 shows a knock event captured both by the PVDF sensor and the commercial accelerometer. The data obtained from the oscilloscope at a 100 kHz sampling frequency were passed through the same 5–10 kHz

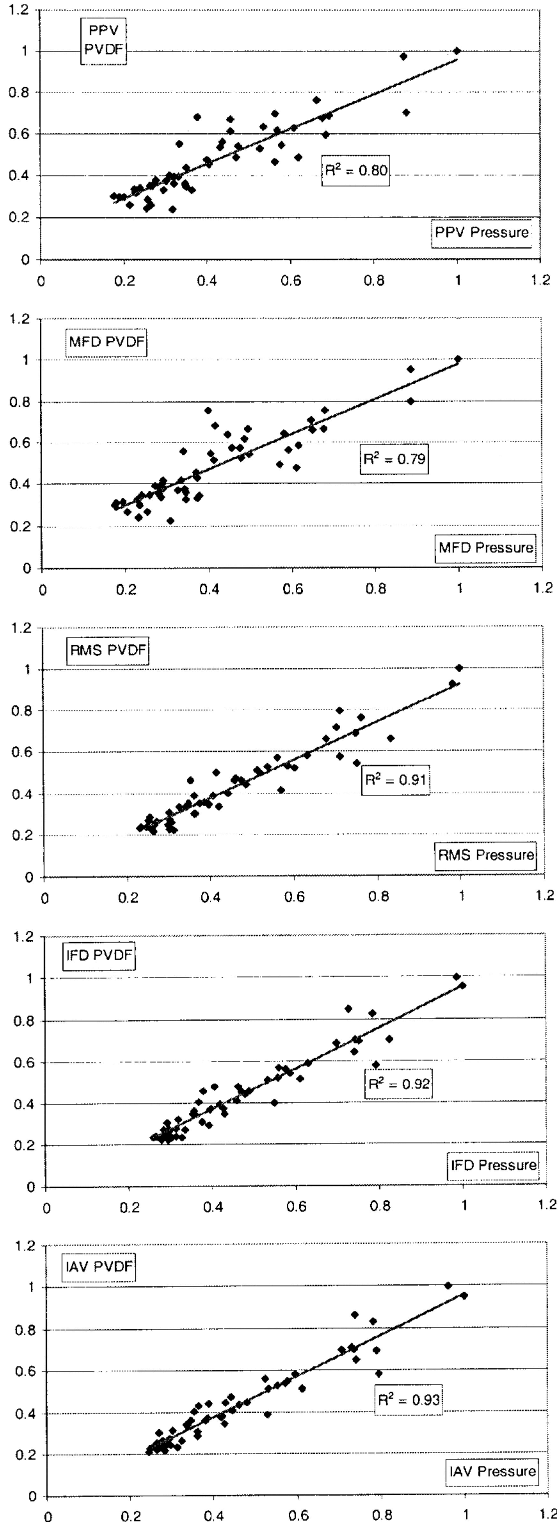

Fig. 6 PVDF knock sensor versus pressure sensor: comparison results

Table 3 Summary of the comparison test between the PVDF sensor and the pressure sensor

	PPV	MFD	RMS	IFD	IAV
Mean KIR	0.52	0.51	0.61	0.59	0.61
SNR ratio	1.14	1.11	1.53	1.44	1.39
Correlation	0.80	0.79	0.91	0.92	0.93

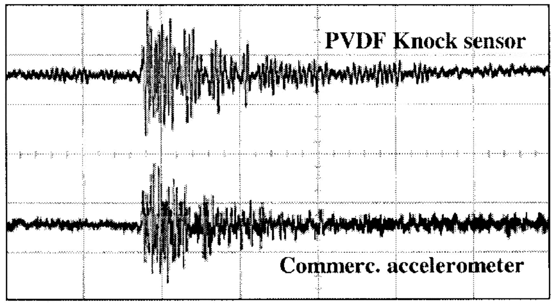

Fig. 7 Knocking captured by PVDF knock sensor and commercial accelerometer (Renault engine, 1500 r/min, 0.89 WOT)

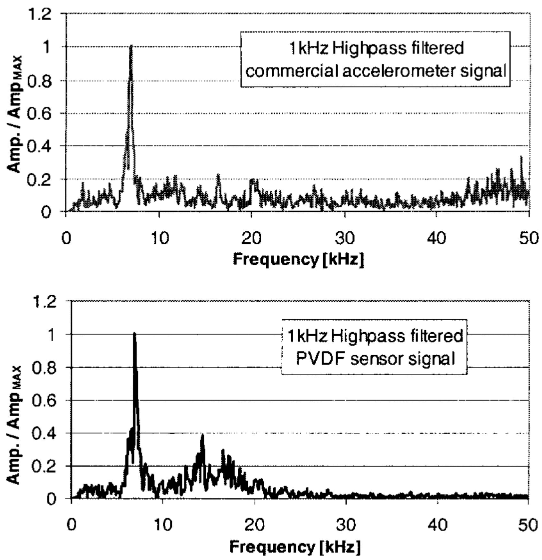

Fig. 8 Power spectra of the high-pass filtered signals (Renault engine, 1500 r/min, 0.89 WOT)

bandpass filter used for the CFR tests, since the power spectra of the 1 kHz high-pass filtered signals revealed the main knocking frequency to be about 7 kHz (Fig. 8); the same result can be obtained by Draper's equation (1), using the series production engine bore $B = 79.5$ mm.

As regards the calculation of KI, an observation window of 50° CA was also considered for these tests. Tables 4 and 5 show the results of the 1500 r/min test, while Tables 6 and 7 refer to the 3000 r/min test.

In the 1500 r/min test, the PVDF knock sensor and the commercial accelerometer measured about the same KI, but the first was characterized by a considerably higher SNR. In the 3000 r/min test the global performance of the PVDF knock sensor with respect to the accelerometer worsened: this is probably caused by the influence of background noise, which becomes heavier and heavier at growing speed.

Table 4 Results of the cylinder 3 knocking test, 1500 r/min at 0.89 WOT (comparison between the PVDF sensor and the commercial accelerometer)

	PPV	MFD	RMS	IFD	IAV
Mean KI ratio	1.05	1.04	1.07	1.02	1.02
SNR ratio	1.69	1.62	1.58	1.42	1.46
Correlation	0.91	0.89	0.98	0.98	0.98

Table 5 Results of the cylinder 2 knocking test, 1500 r/min at 0.89 WOT (comparison between the PVDF sensor and the commercial accelerometer)

	PPV	MFD	RMS	IFD	IAV
Mean KI ratio	1.01	1.08	1.00	1.00	0.98
SNR ratio	1.57	1.53	1.44	1.32	1.36
Correlation	0.82	0.83	0.97	0.98	0.98

Table 6 Results of the cylinder 3 knocking test, 3000 r/min at 0.85 WOT (comparison between the PVDF sensor and the commercial accelerometer)

	PPV	MFD	RMS	IFD	IAV
Mean KI ratio	0.86	0.84	0.98	1.00	1.01
SNR ratio	0.96	0.93	1.18	1.23	1.24
Correlation	0.76	0.73	0.94	0.95	0.95

Table 7 Results of the cylinder 2 knocking test, 3000 r/min at 0.85 WOT (comparison between the PVDF sensor and the commercial accelerometer)

	PPV	MFD	RMS	IFD	IAV
Mean KI ratio	0.91	0.96	0.90	0.93	0.91
SNR ratio	1.02	0.99	1.00	1.01	1.00
Correlation	0.47	0.53	0.75	0.80	0.77

The data presented in Tables 4 to 7 denote a worsening in PVDF knock sensor performance moving from cylinder 3 to 2. This has been attributed to the bonding location of the two sensors: in fact, owing to the limited space available on the Renault engine block, the PVDF knock sensor was placed closer to cylinder 3 than to cylinder 2, while the commercial accelerometer was located equidistant from the two cylinders; for this reason, the PVDF knock sensor was more influenced by the noise induced by cylinder 3 (which affects the cylinder 2 knocking signal) than the noise induced by cylinder 2 (which affects knocking detection on cylinder 3). Therefore, the bonding location of the PVDF knock sensor was favourable for cylinder 3 knocking detection (see Tables 4 and 6) and unfavourable for cylinder 2 knocking detection (see the results in Tables 5 and 7). In spite of the unfavourable positioning of the PVDF sensor compared with the commercial accelerometer during cylinder 2 knocking detection, the correlation between their signals was still satisfactory. The test conducted on the Renault series production engine proved the PVDF-based knock sensor to be competitive with the commercial accelerometer both for knock detection and for knock energy quantification.

The data obtained in the 1500 r/min cylinder 2 knocking test (Table 5) are plotted in Fig. 9, while the results

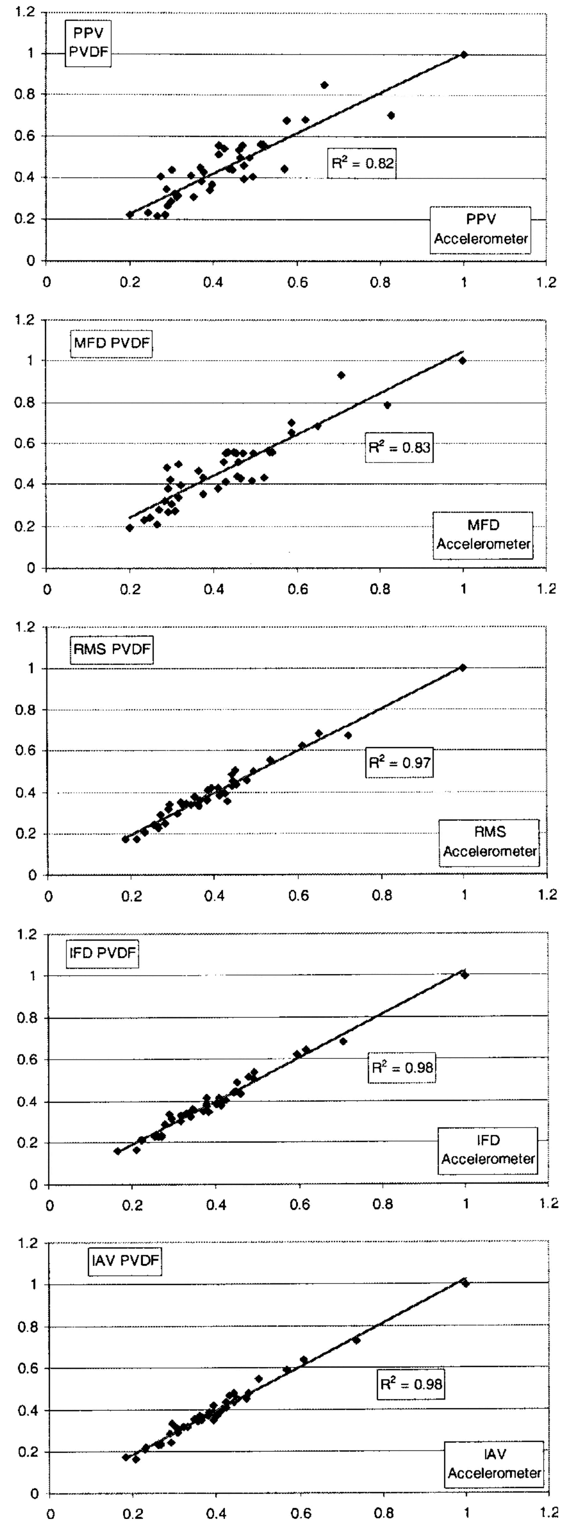

Fig. 9 Relative KI measured during cylinder 2 knock test on the Renault engine (1500 r/min, 0.89 WOT)

of the 3000 r/min cylinder 3 knocking test (Table 6) are presented in Fig. 10. These figures clearly show once again the evaluation criteria subdivision into two categories: PPV and MFD knock intensity definitions obtained a moderate correlation, while RMS, IFD and IAV reached a higher correlation factor.

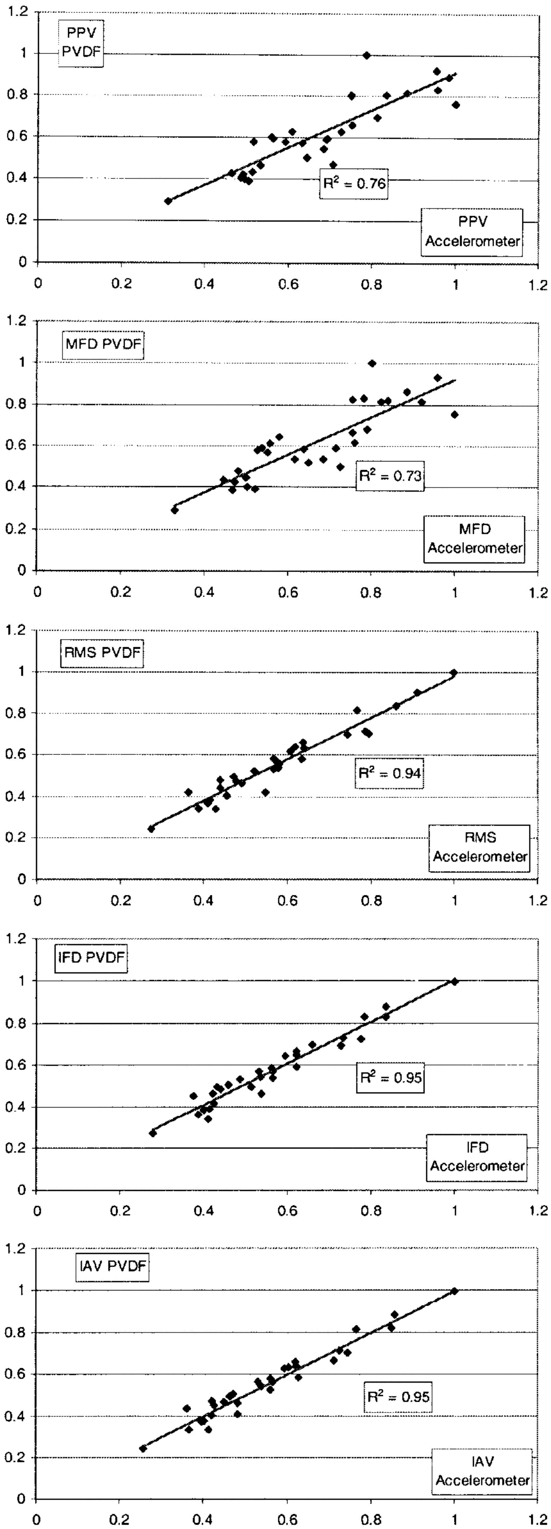

Fig. 10 Relative KI measured during cylinder 3 knock test on the Renault engine (3000 r/min, 0.85 WOT)

4 CONCLUSION

The authors have developed a low-cost automotive knock sensor whose sensing element is a thin washer of PVDF, a polymer with a strong piezoelectric effect.

The sensor has been tested on a CFR spark ignition engine and on a modern series production engine, and its performance, in terms of knock detection, knock energy evaluation and signal-to-noise ratio, has been compared with that of a commercial accelerometer and a pressure sensor.

The results clearly show that PVDF has great potential as a knock detector for spark ignition engines at a very low cost. The PVDF knock sensor, which proved to be suitable both for series production engines and for R&D, worked for several hours without manifesting problems and thermal drift, and, above all, owing to the relatively high voltage field generated by mechanical stress, the use of a charge amplifier was unnecessary.

ACKNOWLEDGEMENTS

This research has been supported by the Italian Ministry for University Research MURST. The support of Renault Italia, in particular Federico Fantozzi, in providing the engine used in the tests, is gratefully acknowledged. The authors would also like to express appreciation to Mr Beniamino Drago for his valuable technical support.

REFERENCES

1 **Baik, S. H.** and **Chun, K. M.** A study on the transient knock control in a spark-ignition engine. SAE paper 981062, 1998.

2 **Beccari, A.** and **Pipitone, E.** Influenza di dosatura ed anticipo d'accensione sulle prestazioni del motore. 55th ATI National Congress, Matera, Italy, 16–20 September 2000.

3 *Bosch Automotive Handbook*, 5th edition, 2000 (SAE).

4 **Heywood, J. B.** *Internal Combustion Engine Fundamentals*, 1988 (McGraw-Hill).

5 **Kaneyasu, M., Kurihara, N., Katogi, K.** and **Tabuchi, K.** An advanced engine knock detection module performs higher accurate MBT control and fuel consumption improvement. 8th International Conference on *Solid-State Sensors and Actuators*, 1995, Vol. 1.

6 **Soelaiman, T. A. F.** and **Kittelson, D. B.** Determining the threshold value of knock intensity for a knock control system in spark ignition engines. 8th International Pacific Conference of Automotive Engineers (IPC-8), Yokohama, Japan, 1995.

7 **Zhang, F., Ge, Y., Huang, Y., Liu, F., Sun, Y.** and **Wu, S.** A micro-processor based adaptive ignition control system.

Proceedings of IEEE International Vehicle Electronics Conference (IVEC '99), 1999.
8 **Chun, K. M.** and **Heywood, J. B.** Characterization of knock in a spark-ignition engine. SAE paper 890156, 1989.
9 **Kinoshita, M., Saito, A., Mogi, K.** and **Nakata, K.** Study on ion current and pressure behaviour with knocking in engine cylinder. *JSAE Rev.*, 2000, **21**.
10 **Hudson, C., Gao, X.** and **Stone, R.** Knock measurement for fuel evaluation in spark ignition engines. *Fuel*, 2001, **80**.
11 **Millo, F.** and **Ferraro, C. V.** Knock in S.I. engines: a comparison between different techniques for detection and control. SAE paper 982477, 1998.
12 **Puzinauskas, P. V.** Examination of methods used to characterize engine knock. SAE paper 920808, 1992.
13 **Rizzoni, G.** and **Samimy, B.** Mechanical signature analysis using time–frequency signal processing: application to internal combustion engine knock detection. *Proc. IEEE*, 1996, **84**(9).
14 **Boubal, O.** Knock detection in automobile engine. *IEEE Instrumn and Measmt Mag.*, 2000.
15 **Konig, D.** Application of time–frequency analysis for optimum non-equidistant sampling of automotive signals captured at knock. Proceedings of IEEE International Conference on *Acoustics, Speech, and Signal Processing, ICASSP-99*, 1996, Vol. 5.
16 **Stankovic, L.** and **Böhme, J. F.** Time–frequency analysis of multiple resonances in combustion engine signals. *Signal Processing*, 1999, **79**.
17 **Rizzoni, G.** and **Chen, X. C.** Detection of internal combustion engine knock using time frequency distributions. In *Proceedings of the 36th Midwest Symposium on Circuits and Systems*, 1993, Vol. 1.
18 **Rizzoni, G.** and **Samimy, B.** Time frequency analysis for improved detection of internal combustion engine knock. *Proceedings of the IEEE International Symposium on Time Frequency and Time Scale Analysis*, 1994.
19 *Piezo Film Sensors Technical Manual*, 1999 (Measurement Specialities Inc.) www.msiusa.com.
20 **Pipitone, E.** and **D'Acquisto, L.** First experience with a piezo film based knock sensor. 2nd International Workshop on *Modeling, Emissions and Control of Automotive Engines*, Salerno, Italy, 4 October 2002.
21 **Plint, M.** and **Martyr, A.** *Engine Testing—Theory and Practice*, 1999 (Butterworth-Heinemann).
22 **Abu-Qudais, M.** Exhaust gas temperature for knock detection and control in spark ignition engine. *Energy Conversion and Managmt*, 1996, **37**(9).
23 **Chun, K. M.** and **Kim, K. W.** Measurement and analysis of knock in a SI engine using the cylinder pressure and block vibration signals. SAE paper 940146, 1994.
24 **Lee, J.-H., Hwang, S.-H., Lim, J.-S., Jeon, D.-C.** and **Cho, Y.-S.** A new knock-detection method using cylinder pressure, block vibration and sound pressure signals from a SI engine. SAE paper 981436, 1998.